

Assessing links between upper atmospheric vorticity patterns and directional changes in hurricane tracks

Stefan Becker · M. L. Bükler · C. J. Matyas · R. V. Rohli

Received: 22 October 2009 / Accepted: 8 February 2010 / Published online: 6 March 2010
© Springer-Verlag 2010

Abstract Links between hurricane track changes and upper atmospheric potential vorticity (PV) anomaly patterns were identified qualitatively and analytically between 1990 and 2005 in the Western Atlantic. Strong track changes of hurricanes, particularly the constellations that triggered northward acceleration of the storm systems, were associated with upper-air PV patterns characterized by strongly positive anomalies to the northeast in combination with weak PV to the north of the system center. Constellations that triggered eventual eastward acceleration were associated with strongly positive PV anomalies to the northwest in combination with weak PV to the northeast of the system center. These results may assist hurricane forecasters and modelers in identifying possible signatures of future tropical cyclone tracks.

1 Introduction

Tropical cyclones have generated severe impacts on civilization including large losses of life, property, and psychological ramifications that are inherent during such catastrophes. They are among the deadliest and costliest natural hazards with total losses in the Atlantic topping \$150 billion combined in 2004 and 2005 (Pielke et al. 2008). Understanding the behavior of tropical cyclones has always been a challenge for scientists. Considerable progress has been made in recent decades in understanding and modeling atmospheric dynamics, enabling researchers to learn more about the internal dynamics of tropical cyclones as well as their interaction with the surrounding environment. The use of dropsondes has further increased knowledge about the internal structure of tropical cyclones (Burpee et al. 1996). Even though much has been learned about the factors that influence the development and propagation of tropical cyclones, the prediction of track still presents great challenges. This is partly due to the complex nonlinear interactions between a tropical cyclone and its surrounding atmosphere, which often lead to significant deviations between observed tracks and the output of dynamical forecast models.

The explanation of tropical cyclone tracks based on key atmospheric variables has been the object of numerous studies. Early observations of tropical cyclone motion led to the conclusion that they move with the steering circulation in which they are embedded (Emanuel 2003). This explains the movement of tropical cyclones from east to west during the earlier stages in their development as a result of the trade wind (easterly) flow. In the late 1940s, additional information on factors impacting cyclone tracks was provided by Davies (1948) and Rossby (1949), who explained the poleward and westward advection of cyclo-

S. Becker (✉)
Department of Geography and Urban Planning,
University of Wisconsin Oshkosh,
Algoma Blvd. 800,
Oshkosh, WI 54901, USA
e-mail: beckers@uwosh.edu

M. L. Bükler
Department of Geography, Western Illinois University,
Macomb, IL, USA

C. J. Matyas
Department of Geography, University of Florida,
Gainesville, FL, USA

R. V. Rohli
Department of Geography and Anthropology,
Louisiana State University,
Baton Rouge, LA, USA

nes as a result of the conservation of vorticity. This phenomenon, also named “beta drift”, is caused by the advection of the background potential vorticity (PV) field by the storm circulation. Beta drift generally causes tropical cyclones to move poleward and westward relative to the motion that they would have if the background PV field were unperturbed by the storms.

In the current study, we analyze potential links between PV anomaly patterns at distances up to 2,500 km from the hurricane centers and changes in the hurricane tracks. The results will contribute to the discussion regarding factors influencing hurricane tracks. We are particularly interested in identifying features in PV patterns that will explain the shift of hurricane track direction from a predominately westward component to a northwestward component and eventually to a northeastward component. The location of this crucial northward acceleration determines if and where a hurricane will make landfall on the US coast. The aim of the study is to analyze whether upper-air PV patterns can explain this acceleration.

1.1 Background: understanding links between atmospheric vorticity and hurricane motion

Many researchers have postulated links between tropical cyclones and vorticity anomalies. One explanation holds that cyclonic circulation advects low-vorticity air northward on the east side of the vortex. This induces an anticyclonic vorticity anomaly to the east. A corresponding cyclonic vorticity anomaly is produced to the west of the vortex. The asymmetric gyres induced by these vorticity anomalies advect the vortex toward the north. Cyclonic advection of the gyres by the vortex itself turns the track toward the northwest (Anthes and Hoke 1975; Carr and Elsberry 1990; Shapiro and Ooyama 1990).

Studies up to the late 1980s and early 1990s were based on the assumption that the vortex flow itself and the surrounding airflow do not vary with height (i.e., barotropic flow). Work on the barotropic theory of hurricane motion was advanced by Holland (1983), Chan (1984), DeMaria (1985), Chan and Williams (1987), and Fiorino and Elsberry (1989). Smith and Ulrich (1990), Smith (1991), and Smith and Weber (1993) developed analytic expressions for the motion of barotropic vortices. After 1 or 2 days of adjustment, an initially symmetric hurricane-like vortex drifts to the northwest at a near-constant speed of a few meters per second (Shapiro and Ooyama 1990). Advection by an environmental wind adds to the vortex motion. For short time intervals, environmental vorticity acts just like the planetary effect; the initially symmetric vortex propagates in the direction of the large-scale vorticity gradient (DeMaria 1985). For longer times, nonlinear interaction between the vortex and the environ-

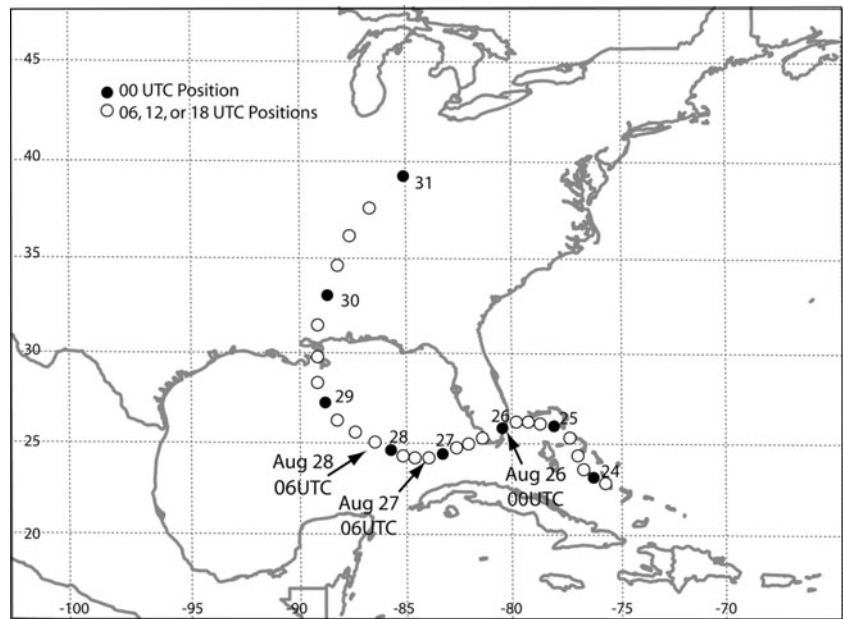
mental wind modifies this simple relationship (Shapiro and Ooyama 1990).

More recent work, however, has revealed that tropical cyclones are baroclinic vortices, and they often occur within large-scale environments that have vertical and lateral wind shear (Emanuel 2003). This shear can have multiple effects on storm motion (Emanuel 2003). Shapiro and Ooyama (1990) pointed toward the connection between shear and background PV. Flatau et al. (1994) examined the interaction between the upper-level anticyclone and the lower-level cyclone. The piecewise inversion technique was used by Wu and Emanuel (1995a, b), Wu and Kurihara (1996), and Shapiro (1996) to evaluate the influence of upper- and lower-level PV anomalies on the motion of several tropical cyclones. These studies emphasized the contribution of upper-level (500 hPa and above) anomalies on the flow that steered the tropical cyclones. Jones (2000) and Smith et al. (2000) described the complex tropical cyclone motion as a result of shear tilting the cyclonic PV anomaly. Shapiro and Franklin (1998) used synoptic-flow cases, incorporating dropwindsonde observations for tropical storms and hurricanes, to deduce the 3-D distribution of PV that contributed to the deep-layer (e.g., 100–1,000 hPa) mean wind that steered the cyclones. They concluded that tropical cyclones are steered either by local (e.g., within 1,000 km of its center) or large-scale (e.g., outside of 2,000 km from its center) PV anomalies.

Wu and Wang (2001) claimed that a difficulty in such approaches is that the technique depends critically on the vertical stability of the atmosphere. They suggested that the study of tropical cyclone motion should be based on the time tendency of PV. They showed in their numerical study without a background flow that the contributions to the motion of the model vortex in the midtroposphere are mainly from the horizontal advection and the diabatic heating terms. A further breakdown of the heating term shows that the asymmetric component of diabatic heating tends to cause a vortex to move toward a region of maximum gradient of asymmetric heating (Wu and Wang 2001). Chan et al. (2002) stated that two fundamental mechanisms are operating: advection by the environmental flow of the relative vorticity associated with the tropical cyclone (the so-called steering) and advective processes that involve the nonlinear interactions among the environmental flow, the planetary vorticity gradient, and the vortex circulation.

Chan et al. (2002) attempted to use the approach of Wu and Wang (2001) to explain the motion of actual tropical cyclones. They found that the diabatic heating term appears to be important in slow-moving tropical cyclones and those with oscillatory motion or sudden track changes. Otherwise, the horizontal advection term is generally dominant. They concluded that the motion of a tropical cyclone apparently follows the area of maximum azimuthal wave-

Fig. 1 Track of Hurricane Katrina in 2005



number 1 PV, which is composed mainly of the horizontal advection and diabatic heating terms. Furthermore, they noticed that because the contribution of heating toward motion is through its horizontal gradient, the motion vector was found in many cases to be toward the edge of the heaviest convection, a result previously found by Lajoie (1976) from examination of satellite imagery.

Zhang et al. (2007) stated that the track largely depends on the large-scale environment, which has become more and more predictable with rapid advances in numerical weather prediction models and better observing systems.

Several models have led the way in improving tropical cyclone track forecasts. An early statistical approach to link tracks to various external forces has been pursued by the Climatology and Persistence (CLIPER) model, which is a multiple regression-based model that best utilizes the persistence of the current motion and also incorporates climatological track information (Aberson 1998). CLIPER has been outperformed by dynamical models since the 1980s. The statistical–dynamical National Hurricane Center 1998 model incorporates statistical relationships between storm behavior and predictors obtained from dynamical

Fig. 2 Track of Hurricane Rita in 2005

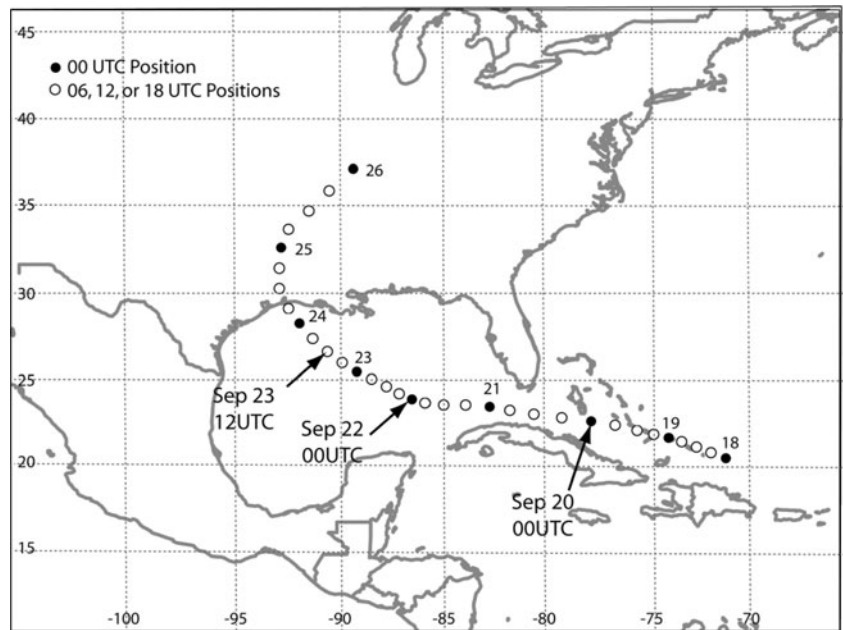
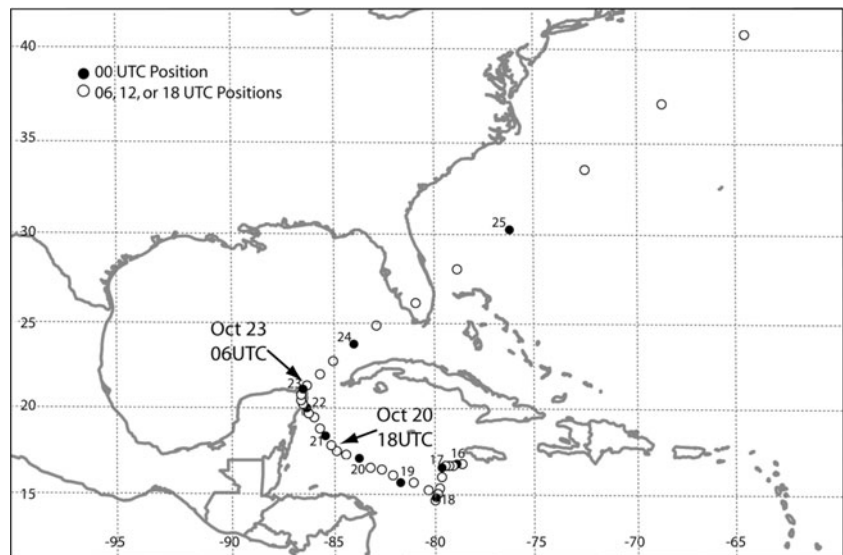


Fig. 3 Track of Hurricane Wilma in 2005



model forecasts, such as the deep-layer-mean global forecast system (GFS) geopotential height fields (averaged from 1,000 to 100 hPa; Rhome 2007). An additional approach in linking tracks to external forces is represented by trajectory models such as the beta and advection model (BAM; Marks 1992). While trajectory models utilize information from dynamical models to represent the prevailing flow, they do not allow the cyclone to interact with the surrounding atmosphere. BAM is a trajectory model that utilizes vertically averaged horizontal winds at different levels from the GFS to compute the trajectories. Additional information on these and various other models can be found in Rhome (2007).

Over the past decade, significant progress has been made in short-range (up to 5-day) track forecasts of tropical cyclones. The current-day average 48-h forecast position is as accurate as a 24-h track forecast 10 years ago (Franklin 2005). Yet, room for improvement still exists. Even though many of the effects mentioned above are contained in advanced numerical forecast models, such as the Princeton/Geophysical Fluid Dynamics Laboratory (GFDL) tropical cyclone prediction model (Bender et al. 1993; Kurihara et al. 1998), it is obvious that the internal and external forces that determine the track of a tropical cyclone have not yet been modeled successfully. In addition, since observations are not taken at every location around the world, the quality

Fig. 4 Simplified, schematic illustration of upper tropospheric PV patterns associated with hurricane track directional changes

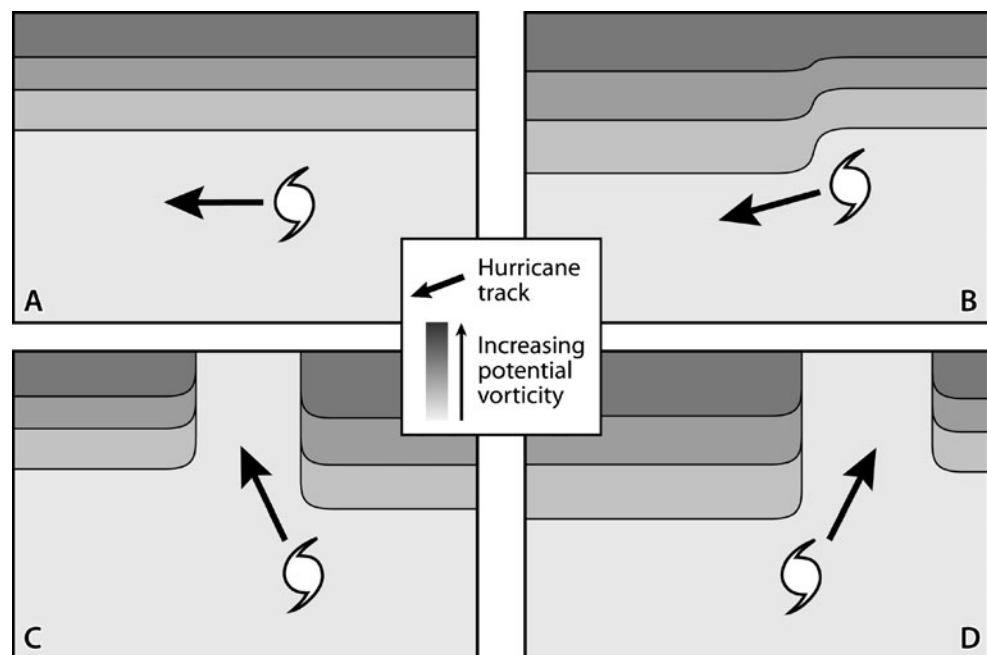
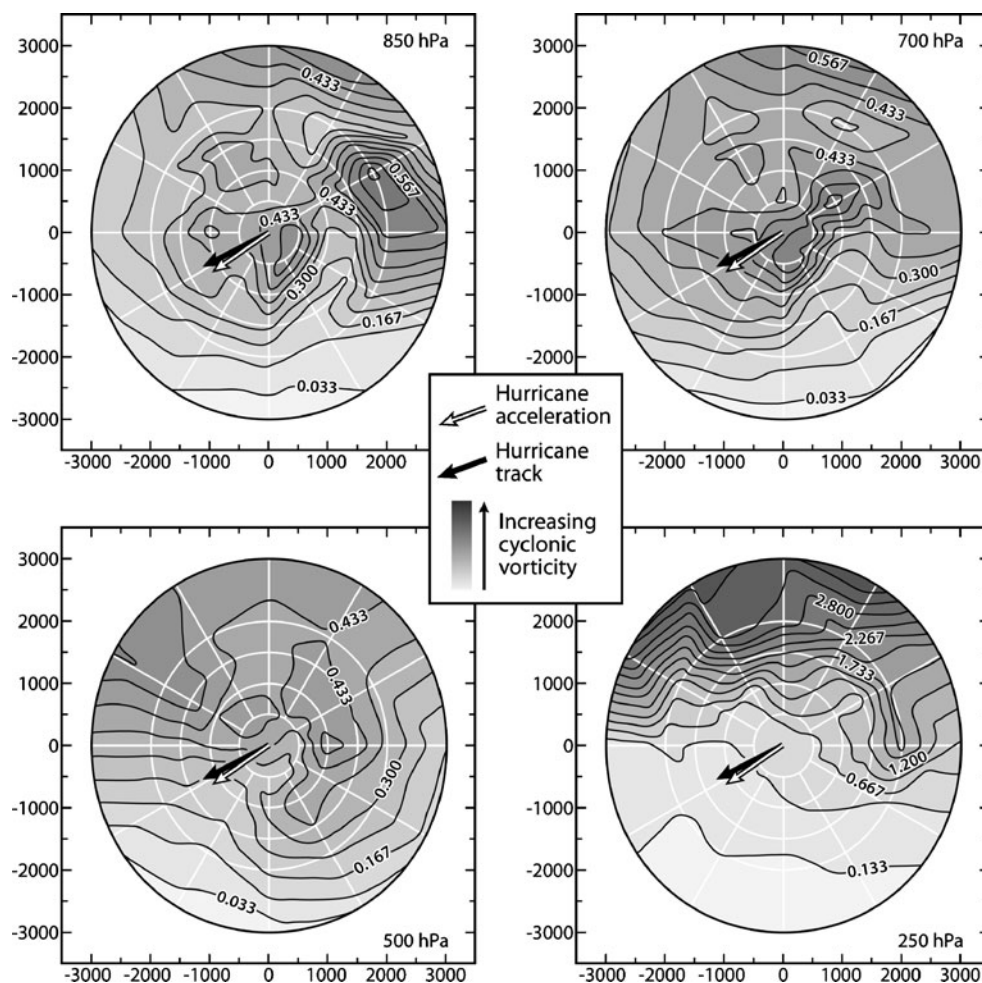


Fig. 5 PV anomalies in the environment of Hurricane Katrina on 26 August 2005, 0000 UTC. Each panel shows spatially interpolated PVs at 850 (upper right), 700 (upper left), 500 (lower left), and 250 hPa (lower right). The black arrow is the motion vector; the white arrow is the acceleration vector. Data are derived from the NCEP/NCAR reanalysis data set. Note the varying contour interval in the panels



of model initialization can vary tremendously. This is one of the primary sources of uncertainty and forecast errors within dynamical models. Errors in the initial state of a model tend to grow with time during the actual model forecast (Rhome 2007). Reflections on the performance of the GFDL model during the recent tropical cyclone seasons are found in Bender et al. (2007). To improve the performance of tropical cyclone track models further, four components are necessary: (a) increased computer power, (b) higher-resolution models, (c) a better capture of the initial structure of the tropical cyclone, and (d) a better representation of the physics, especially that dealing with the surface of the ocean and the exchange of energy, matter, and momentum fluxes from the surface of the ocean to the tropical cyclone (Online Interview with Morris Bender, 18 July 2007, available at <http://www.oar.noaa.gov/podcast/audio2007/bender.html>).

2 Data and methods

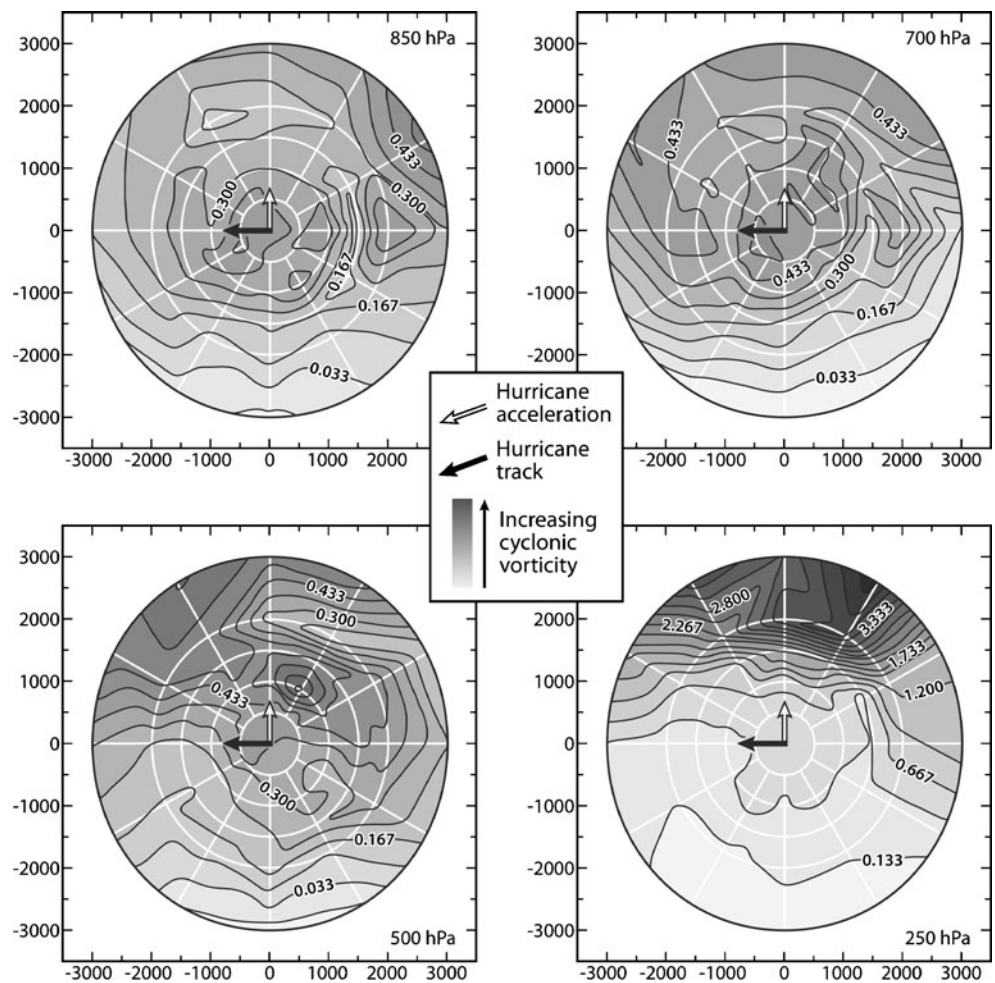
Track and intensity data are available from the National Hurricane Center's North Atlantic hurricane database for

211 tropical cyclones documented in the Western Atlantic basin between 1990 and 2005. Of these, 95 attained tropical or extratropical storm status while 116 attained hurricane status and were analyzed in this project. The data set contains the position and intensity for every 6 h; intensity is represented by the minimum sea level pressure and the mean 1-min sustained surface wind throughout the life of each storm. We utilized the position data to calculate directional changes in hurricane paths which were subsequently linked to PV anomaly patterns.

The external atmospheric environmental features (up to 2,500 km distance and in 12 directions from the eye) were derived from the National Centers for Environmental Prediction (NCEP) reanalysis data sets. The National Oceanic and Atmospheric Administration (NOAA) Climate Diagnostics Center provides six hourly data on temperatures, horizontal and vertical winds, and pressure patterns which are all available for various altitudes since 1948. The NOAA (NCEP/National Center for Atmospheric Research (NCAR)) reanalysis data set has a 2.5° spatial resolution.

Much insight into the nature of rotating, stratified flows can be obtained by considering the concept of PV. Given

Fig. 6 PV anomalies in the environment of Hurricane Katrina on 27 August, 0600 UTC



the widely discussed links between upper atmospheric circulation patterns (ridges and troughs) and cyclone tracks, we expect upper-air PV anomalies to be valuable deterministic factors for hurricane tracks. Thus, from the available data, we calculated PV values for the 850-, 700-, 500-, and 250-hPa pressure levels. We calculated PV values for each 6-h time step over the life of each hurricane.

The calculation of PV is based on the algorithm of Ertel (1942). Ertel’s generalized 3-D PV is formulated as the density (ρ)-weighted dot product of the 3-D vorticity vector $\vec{\omega}$ and the 3-D gradient of potential temperature (θ).

$$PV = \rho^{-1} \vec{\omega} \cdot \nabla \theta.$$

In atmospheric applications, this formulation is usually simplified to account for only absolute vertical vorticity (relative (ζ) and planetary (f)) and the vertical gradient of θ (in isobaric coordinates). Therefore, we calculated PV, using the NCEP data on the four pressure levels, as the product of gravity (g), the vertical potential temperature

gradient with respect to pressure ($\partial\theta/\partial p$), the vertical component of ζ and f :

$$PV = -g \frac{\partial\theta}{\partial p} (\zeta + f)$$

Vertical vorticity was approximated with a horizontal center difference of the u and v components of the wind:

$$\zeta = \frac{\partial v}{\partial x} - \frac{\partial u}{\partial y}$$

$$\zeta \cong \frac{v_{x+1} - v_{x-1}}{2\Delta x} - \frac{u_{y+1} - u_{y-1}}{2\Delta y}$$

θ was calculated using temperature at each of the 17 pressure levels available using Poisson’s equation:

$$\theta = T \times (1000/P)^{0.287}$$

where T = air temperature in K and P = air pressure in hectopascals and 0.287 is $R_d/c_p \cdot \frac{\partial\theta}{\partial p}$, the vertical potential temperature gradient with respect to pressure, was approx-

imated with a center difference using the pressure level above and below our levels of interest. In the upper troposphere, by definition, high values of PV are associated with either high static stability ($\partial\theta/\partial p \gg 0$), high inertial stability ($\zeta + f \gg 0$), or both.

The assessment of potential links between PV patterns and hurricane track changes was done visually for all hurricanes in the Atlantic from 1990 to 2005. To facilitate the analysis, PV values were spatially interpolated for each level. In addition to the hurricane track and interpolated PV values, the set of illustrations that we produced contains information on the direction and distance that the hurricane center will travel within the subsequent 6 h. Also, the illustrations contain information about the hurricane acceleration, which refers to the first derivate of the translational movement and can be interpreted as translational changes at the respective time step. We generalized the PV values into four basic patterns that correspond to directional changes in hurricane tracks. Specifically, we analyzed the tracks of the 116 cyclones which attained hurricane status between 1990 and 2005. We identified the hurricanes which turned toward and maintained a northwestern, southwestern, or northeast-

ern track direction for at least 18 consecutive hours. We analyzed the related upper and lower tropospheric PV patterns for these time periods and visually identified characteristic common structures.

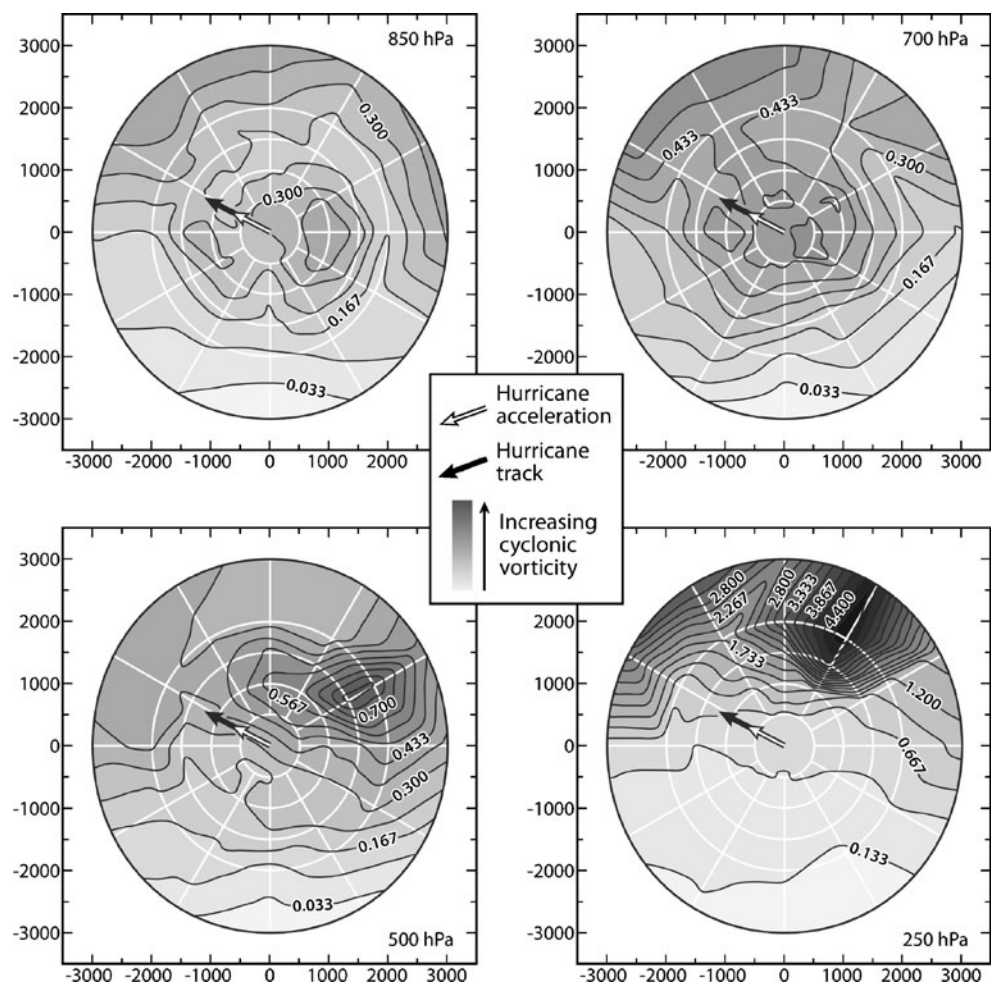
We will demonstrate the findings through three case studies from the 2005 Atlantic hurricane season.

3 Case studies

3.1 Case study 1: Katrina 2005

Hurricane Katrina was the costliest as well as one of the deadliest hurricanes in the history of the USA. It started as a tropical depression over the southeastern Bahamas on 23 August 2005. Knabb et al. (2006a) explain the hurricane track based on upper-air circulation: Initially, the storm moved northwestward within a weakness in the lower tropospheric subtropical ridge. With increasing intensity on 24 August, Katrina came under the influence of a strengthening middle to upper tropospheric ridge over the northern Gulf of Mexico and southern USA which turned it

Fig. 7 PV anomalies in the environment of Hurricane Katrina on 28 August, 0600 UTC



westward on 25 August toward southern Florida. Later, the ridge produced northeasterly middle- to upper-level tropospheric flow that forced Katrina to turn west-southwestward as it neared southern Florida. The ridge that kept Katrina on a west-southwestward track over the Florida peninsula and southeastern Gulf of Mexico shifted eastward toward Florida, while a midlatitude trough amplified over the north-central USA. This evolving pattern resulted in a general westward motion on 27 August and a turn toward the northwest on 28 August when Katrina moved around the western periphery of the retreating ridge. Katrina turned northward around the ridge over Florida early on 29 August and tracked toward the northern Gulf coast (Fig. 1).

generally toward the west, the low-level center steadily reformed to the north, resulting in a west-northwestward motion. The storm strengthened rapidly and turned more westward early on 20 September along the southern periphery of a deep-layer ridge positioned over the western Atlantic and Florida. Rita proceeded westward into the southeastern Gulf of Mexico as a category 3 hurricane early on September 21. On September 22, it turned toward the west-northwest around the western extent of the middle- to upper-tropospheric ridge centered over the southeastern USA. Rita rounded the western periphery of the deep-layer ridge and turned toward the northwest on September 23 (Fig. 2).

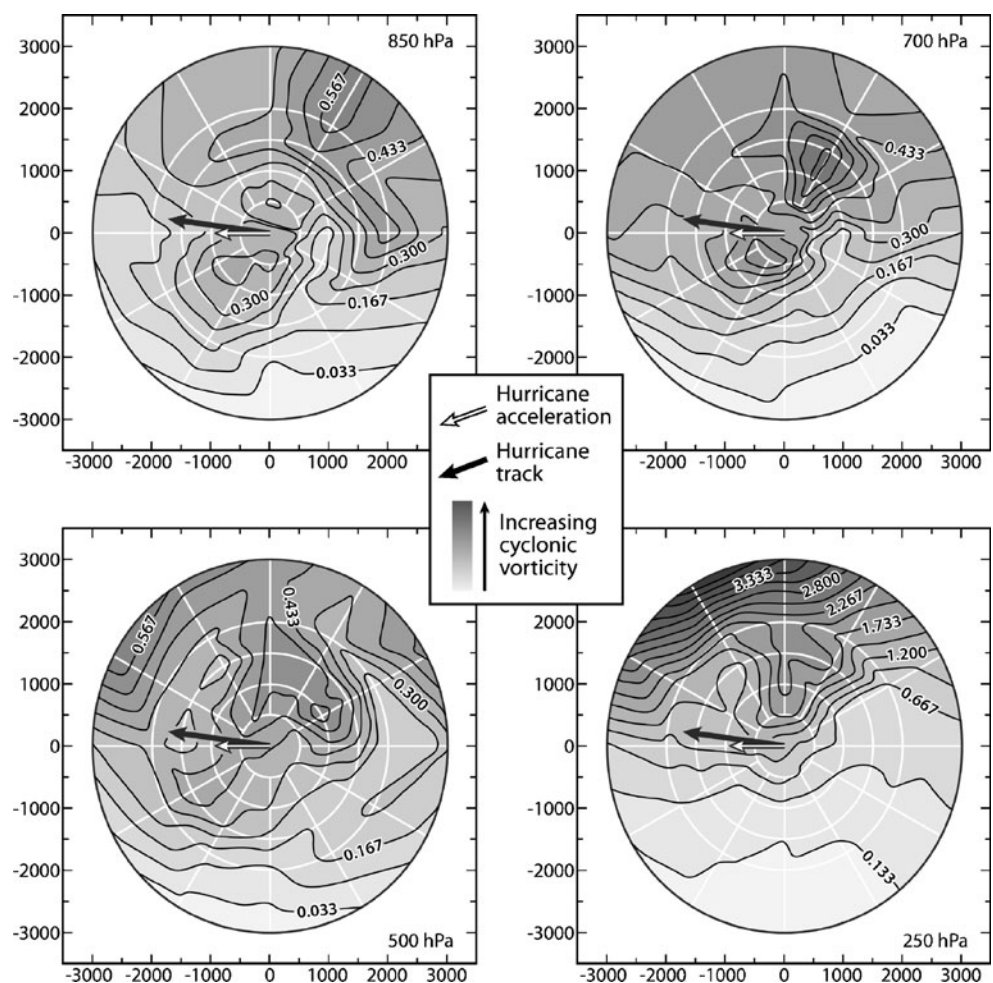
3.2 Case study 2: Rita 2005

Knabb et al. (2006b) explain Rita’s track: A tropical depression is estimated to have formed by 0000 UTC 18 September approximately 130 km east of Grand Turk in the Turks and Caicos. On 18 and 19 September, Rita moved toward the west-northwest over the Turks and Caicos and the southeastern Bahamas. While the steering flow was

3.3 Case study 3: Wilma 2005

Pasch et al. (2006) explain Wilma’s track: The formation of a tropical depression centered about 350 km east-southeast of Grand Cayman was confirmed on October 15. A weak and ill-defined steering flow prevailed for several days, with a 500 hPa high covering the Gulf of Mexico and another midtropospheric anticyclone located well to the

Fig. 8 PV anomalies in the environment of Hurricane Rita on 20 September 0000 UTC

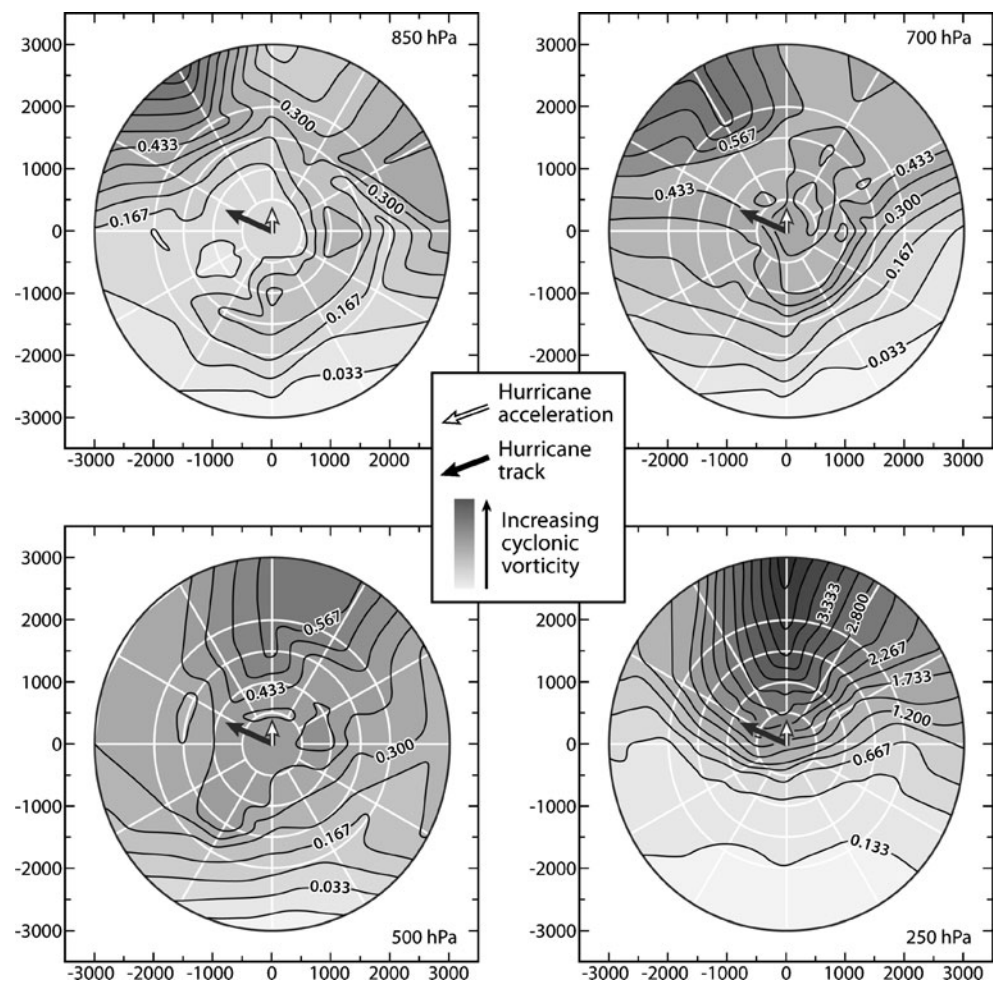


east–northeast of the tropical cyclone. The depression moved slowly and erratically westward to west–southwestward for a day and then drifted south–southwestward to southward. On October 18, Wilma turned toward the west–northwest and, while doing so, strengthened into a hurricane. Later that day, a remarkable, explosive strengthening episode began and continued through early on 19 October. By 21 October, as midlevel ridging to the northeast of Wilma increased somewhat and a series of shortwave troughs in the westerlies began to erode the high over the Gulf of Mexico, the hurricane turned toward the northwest and north–northwest, taking aim at the Yucatan Peninsula of Mexico. On 22 October, the midtropospheric high pressure area to the north of Wilma essentially dissipated, and the hurricane moved slowly northward, crossing and severely battering the extreme northeastern Yucatan peninsula. A vigorous midtropospheric trough, moving eastward from the central USA, provided an increasingly strong southwesterly steering current that accelerated Wilma northeastward toward southern Florida (Fig. 3).

4 Results and discussion

Based on the analysis of hurricanes between 1990 and 2005, we observed characteristic features in the upper-air PV fields that are typically associated with the shift of hurricane direction from a predominately westward to a northward component and eventually to a northeastward direction. The correlations were particularly evident with PV fields at the 250-hPa level. Many track changes were associated with concurrent PV patterns at the 250- and 500-hPa level. Figure 4 is a highly simplified, schematic illustration of upper-air PV patterns that were linked to certain track directional changes. Weakly defined PV anomaly patterns or strongly developed PV patterns to the north of the hurricane center are typically not associated with track changes toward the north but rather with a progression of the system in a western or even southwestern direction (upper left panel a). A generally well-developed pattern of PV anomalies in the north with particularly strong and far south reaching high PV fields in the northwest typically leads to a track in southwestern directions (upper right panel b). A well-developed pattern of

Fig. 9 PV anomalies in the environment of Hurricane Rita on 22 September 0000 UTC



positive PV anomalies to the northeast of the system typically leads to its northward acceleration, particularly when it is accompanied by relatively weak PV in the north (lower left panel c). A strongly developed PV pattern to the northwest of the system in association with weak PV in the northeast is often associated with recurving of the track in a northeastern direction (lower right panel d). In all cases, the hurricane had a tendency to accelerate toward lower inertial and/or static stability in the upper troposphere. This is consistent with the hurricane optimizing inertial available kinetic energy (Mecikalski and Tripoli 1998), where convection will tend toward a region of “least resistance” in the upper troposphere.

Additionally, while we did not find as strong a correlation of hurricane motion with the PV field at 850 or 700 mbar, it is known that low-level (positive) PV anomalies can be indicative of thermal maxima near the surface (Hoskins et al. 1985; Ma et al. 2002). There is some indication in our study that the hurricanes also had a tendency to migrate toward these features.

A total of 56 of the 116 hurricanes shifted toward or remained on a persistent northwestward track while they

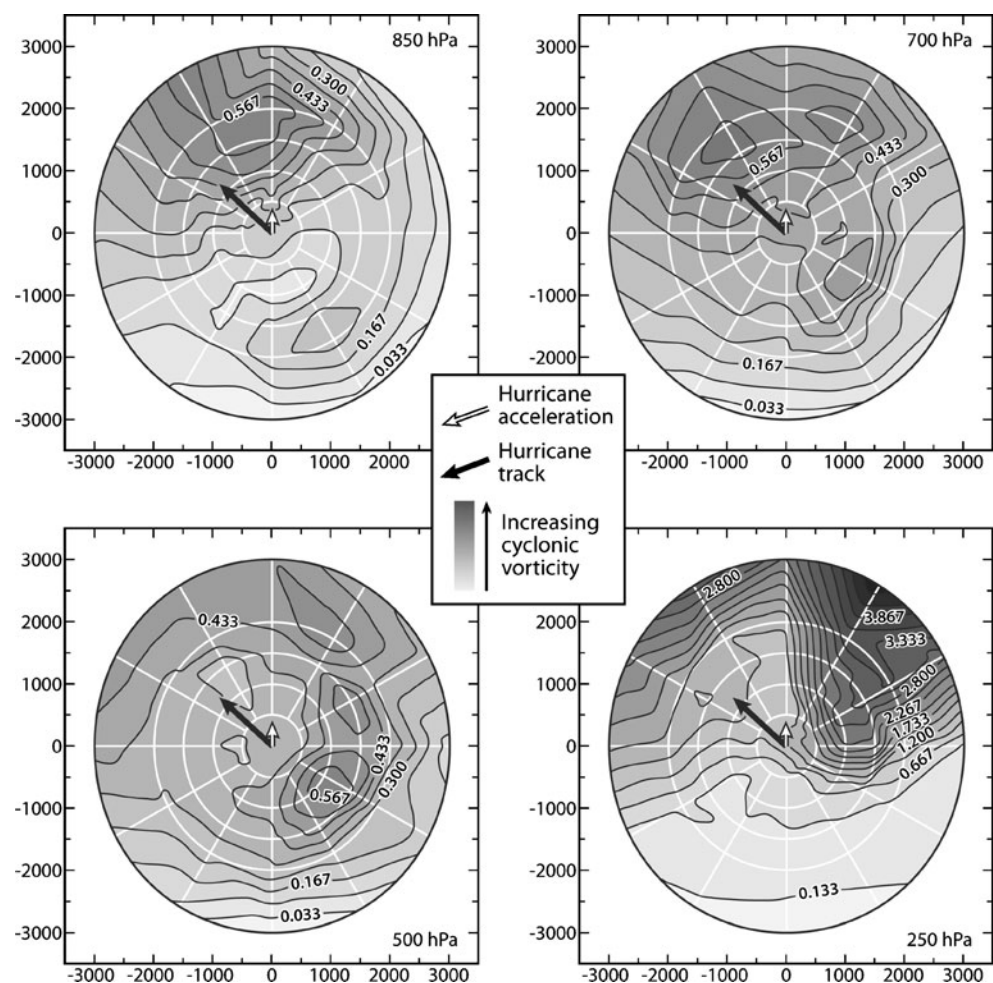
attained or maintained hurricane status. Of these, 44 (78%) of these upper-air PV patterns resemble lower left in Fig. 5. Of the 116 hurricanes, 76 shifted toward or remained on a persistent northeastward track while they attained or maintained hurricane status. For 66 (86%) of these, upper-air PV patterns resemble panel d in Fig. 4.

These generalized observations will be specified by using the case studies below.

4.1 Case study 1: Katrina 2005

For the beginning stages of Katrina on 23 to 24 August, we observed PV patterns at the 750-, 500-, and 250-hPa levels matching panel c in Fig. 4, which explains the northwestward progression of the system. On 25 to 26 August, the PV patterns at the 500 and 250 hPa changed to the “a” and “b” schemes. Given that the system had intensified in the meantime to a tropical storm and a hurricane, it is meaningful to relate its track to the upper atmospheric patterns from that point forward. It can be seen in Fig. 5 that the PV anomalies on 26 August 0000 UTC at the 500- and 250-hPa levels did not favor the northward acceleration

Fig. 10 PV anomalies in the environment of Hurricane Rita on 23 September 1200 UTC



of the system and the hurricane progressed on its southwestern track (panel b in Fig. 4).

The upper-air PV pattern in the vicinity of the storm system, which has intensified in the meantime to a category 2 hurricane, changed significantly on 27 August 0600 UTC (Fig. 6). A strongly developed positive PV developed to the northeast of the system with a slight weakening of this pattern to the northwest. This constellation, which intensified during subsequent hours, coincided with the northward acceleration of the hurricane. This coincided with the time at which the storm system turned from a southwestern to a northwestern direction.

On 28 August, a dominant PV pattern at the 500- and 250-hPa levels closely resembles panel c in Fig. 4 and was associated with a further northward progression of the hurricane (Fig. 7). The lower tropospheric PV maximum to the northwest of the storm system (particularly at the 700-hPa level) further contributes to the explanation of the track change. For the next hours, a further intensification of this constellation occurred. Throughout 29 August, the upper-air PV patterns shifted to a constellation that resembles panel d in

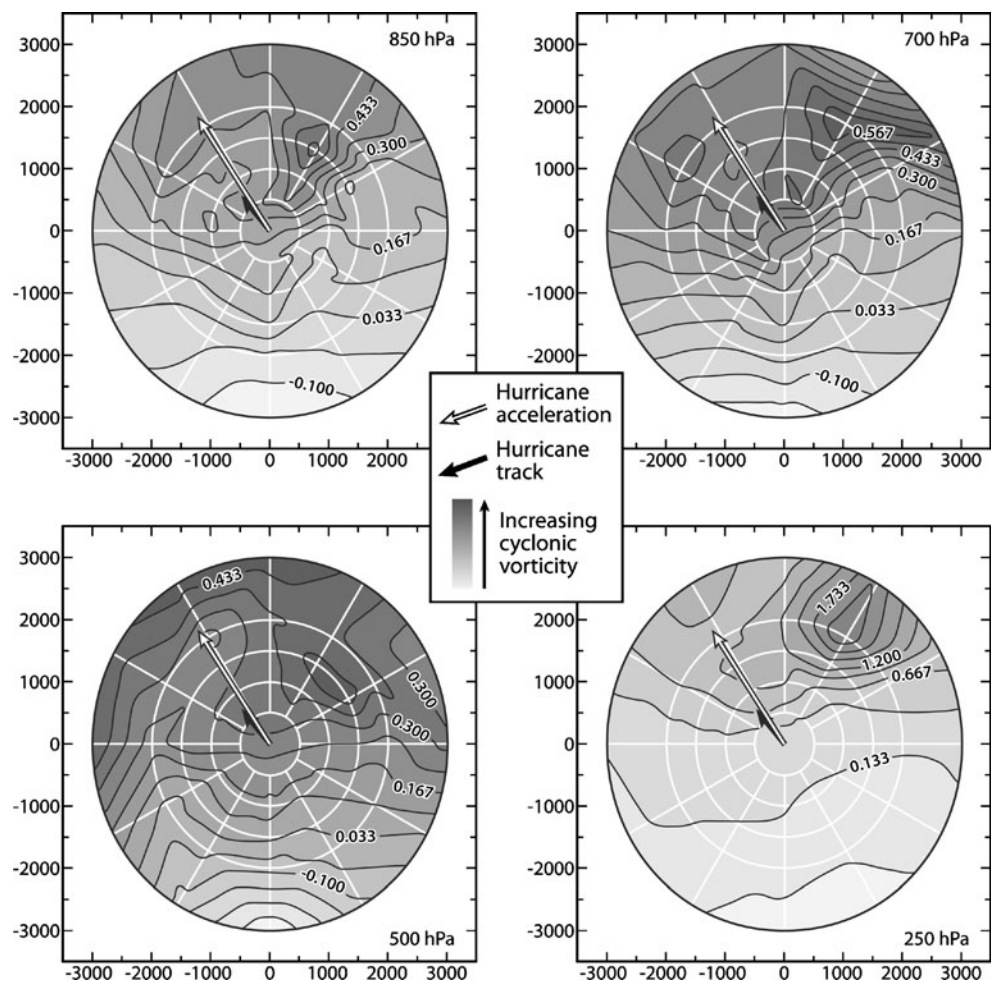
Fig. 4. The associated hurricane track turned to a northeastward direction.

4.2 Case study 2: Rita 2005

During Rita's early stages, the upper-air PV pattern would have clearly facilitated the system's northward progression if Rita had already attained hurricane intensity. When Rita finally developed sufficient intensity on 20 September, strongly developed positive PV anomaly fields occurred at 500- and 250-hPa levels, keeping the hurricane on the predominately westward track (Fig. 8, reminiscent of panel a in Fig. 4).

This pattern did not change significantly during the following hours. For 21 September and particularly the day after, positive PV anomaly fields occurred farther to the northeast of the hurricane center (Fig. 9). This phenomenon can be explained by the hurricane center migrating westward in the south of a relatively stationary and well-developed upper-air trough between 20 and 22 September. The intensification of the northeastern upper-air PV

Fig. 11 PV anomalies in the environment of Hurricane Wilma on 18 October 0600 UTC



anomaly explains the turning point of the hurricane during 22 September which eventually led to an increased northward acceleration and a northwestward track. The lower tropospheric PV maximum to the northwest of the storm system also contributes to the explanation of the track change. However, a fully developed panel c pattern had not yet occurred, as no gap existed between northeastern and northwestern positive PV centers.

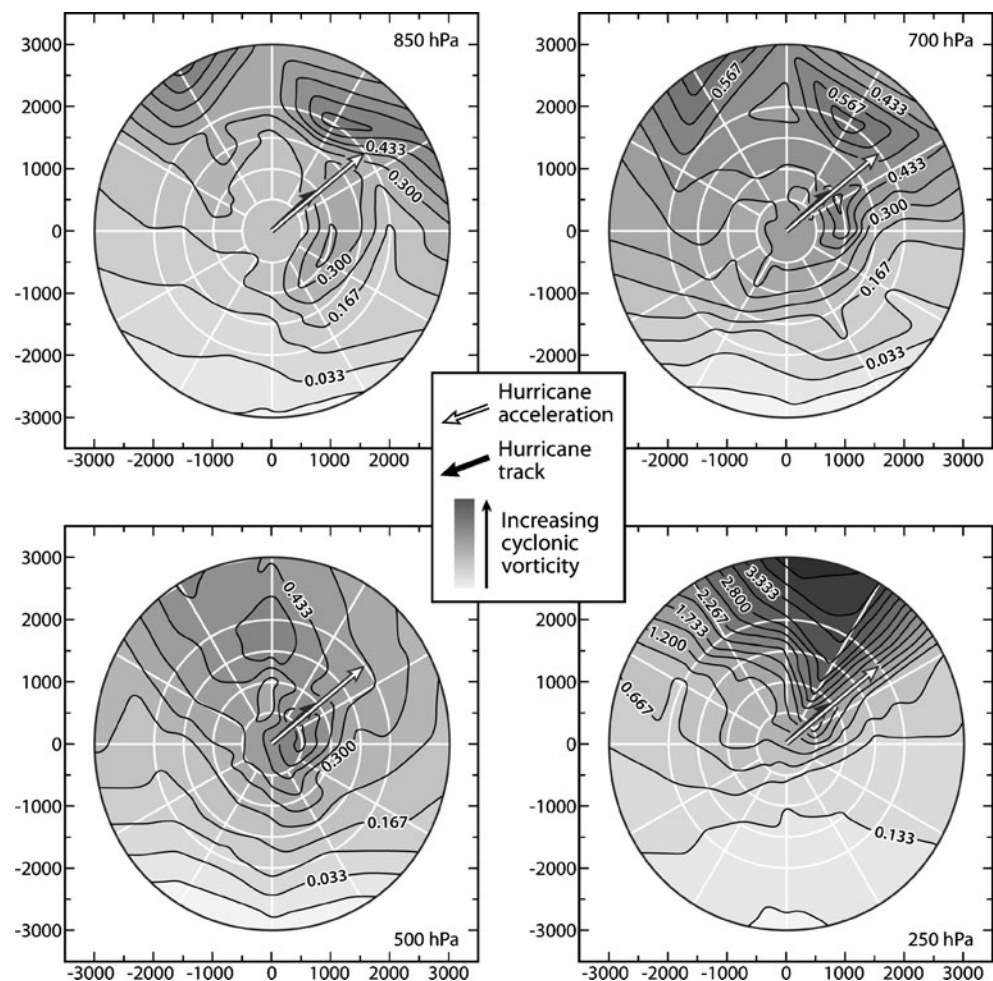
On 23 September, a fully developed lower left constellation formed (Fig. 10), coincident with a lower tropospheric PV maximum in the northwest of the storm center and consequently a further significant northward acceleration of the hurricane. The ridge between the two upper-air positive PV anomaly fields to the northwest and northeast of the hurricane center intensified during the following hours and facilitated the change of the hurricane track onto a northward direction. During 24 September, the storm transitioned to a lower right constellation which was accompanied by a shift of the hurricane track onto the northeastward direction.

4.3 Case study 3: Wilma 2005

The study of upper-air PV anomaly patterns did not yield any conclusive links to the rather erratic track of Wilma during its initial stages. The 250-hPa pattern on 16 to 17 October would have promoted a northwestward track if the system had already intensified to hurricane status; PV patterns at the lower levels are less conclusive but obviously did not promote this direction. A significant change can be observed from 18 October onward. By then, the system had matured to a tropical storm and PV patterns at the 500- and 250-hPa levels (Fig. 11, closely resembling panel c in Fig. 4) triggered the northwestward progression of the system.

During the following days, the distinct positive PV anomaly at the 250-hPa level to the north of the system, which had by then developed into a major hurricane, would allow for both scenarios—the continued northwestward progression and the recurving toward the northeast. The hurricane center continued its northwestward progression

Fig. 12 PV anomalies in the environment of Hurricane Wilma on 23 October 0600 UTC



until 22 August when it encountered strong positive PV anomalies at the 500- and 250-hPa levels nearly reaching the center of the system itself in the region of the Yucatan peninsula. This was associated with a particularly slow progression of the system and eventually the shift to a northeastward direction. Figure 12 shows that the hurricane center had migrated northeastward and therefore avoided the 250-hPa positive PV anomaly field. In addition, the lower tropospheric high PV anomalies to the northeast of the storm system contribute to the explanation of the track changes.

5 Conclusion

The aim of the study was to assess potential links between the upper atmospheric PV patterns and track changes in tropical cyclones. The case studies alone are not sufficient to contribute considerably to the explanation or forecast of hurricane tracks in general. However, the case studies clearly show that turning points in hurricane tracks are associated with characteristic PV patterns particularly at the 250- and 500-hPa levels, and the generalized results from the other hurricane tracks examined support our findings. Given that strongly positive upper-air PV anomalies can generally be related to upper-air troughs, we can interpret some of the observations by our knowledge about hurricane steering through upper-air troughs as discussed for the case studies. Tropical disturbances that have matured to hurricane intensity will generally be directed along the upper-air ridges away from trough axes. Because upper-level ridges are usually associated with weak inertial and static stability, it is not surprising that organized convection in a tropical cyclone will tend to migrate in that direction. The model shown in Fig. 4 can serve as a foundation for subsequent studies to link the observed track changes to upper-air PV patterns stochastically.

References

- Aberson SD (1998) Five-day tropical cyclone track forecasts in the North Atlantic basin. *Weather Forecast* 13:1005–1015
- Anthes RA, Hoke JE (1975) Effect of horizontal divergence and latitudinal variation of Coriolis parameter on drift of a model hurricane. *Mon Weather Rev* 103:757–763
- Bender MA, Ross RJ, Tuleya RE, Kurihara Y (1993) Improvements in tropical cyclone track and intensity forecasts using the GFDL initialization system. *Mon Weather Rev* 121:2046–2061
- Bender MA, Ginis I, Tuleya R, Thomas B, Marchok T (2007) The operational GFDL coupled hurricane-ocean prediction system and summary of its performance. *Mon Weather Rev* 135:3965–3989
- Burpee RW, Franklin JL, Lord SJ, Tuleya RE, Aberson SD (1996) The impact of omega dropwindsondes on operational hurricane track forecast models. *B Am Meteorol Soc* 77:925–933
- Carr LE, Elsberry RL (1990) Observational evidence for predictions of tropical cyclone propagation relative to environmental steering. *J Atmos Sci* 47:542–546
- Chan JC-L (1984) Observational study of the physical processes responsible for tropical cyclone motion. *J Atmos Sci* 41:1036–1048
- Chan JC-L, Williams RT (1987) Analytical and numerical studies of the beta-effect in tropical cyclone motion, Pt. 1. Zero mean flow. *J Atmos Sci* 44:1257–1265
- Chan JC-L, Ko FMF, Lei YM (2002) Relationship between potential vorticity tendency and tropical cyclone motion. *J Atmos Sci* 59:1317–1336
- Davies TV (1948) Rotary flow on the surface of the earth. Part I. Cyclostrophic motion. *Philos Mag* 39:482–491
- DeMaria M (1985) Tropical cyclone motion in a nondivergent barotropic model. *Mon Weather Rev* 113:1199–1210
- Emanuel K (2003) Tropical cyclones. *Annu Rev Earth Planet Sci* 31:75–104
- Ertel H (1942) Ein neuer hydrodynamischer Wirbelsatz. *Meteorol Z* 59:277–281
- Fiorino M, Elsberry RL (1989) Contributions to tropical cyclone motion by small, medium, and large scales in the initial vortex. *Mon Weather Rev* 117:721–727
- Flatau M, Schubert WH, Stevens DE (1994) The role of baroclinic processes in tropical cyclone motion: the influence of vertical tilt. *J Atmos Sci* 51:2589–2601
- Franklin JL (2005) 2004 National Hurricane Center verification report. 57th Interdepartmental Hurricane Conference, Miami, FL [Updates are available on the official National Hurricane Center website: National Hurricane Center (NHC), www.nhc.noaa.gov/verification]
- Holland GJ (1983) Tropical cyclone motion: environmental interaction plus a beta-effect. *J Atmos Sci* 40:328–342
- Hoskins BJ, McIntyre ME, Robertson AW (1985) On the use and significance of isentropic potential vorticity maps. *Q J R Meteorol Soc* 111:877–946. doi:10.1256/smsqj.47001
- Jones SC (2000) The evolution of vortices in vertical shear. Part III: baroclinic vortices. *Q J R Meteorol Soc* 126:3161–3185
- Knabb RD, Rhome JR, Brown DP (2006a) Tropical cyclone report—Hurricane Katrina. National Hurricane Center. Retrieved from <http://www.nhc.noaa.gov>
- Knabb RD, Brown DP, Rhome JR (2006b) Tropical cyclone report—Hurricane Rita. National Hurricane Center. Retrieved from <http://www.nhc.noaa.gov>
- Kurihara Y, Tuleya RE, Bender MA (1998) The GFDL hurricane prediction system and its performance in the 1995 hurricane season. *Mon Weather Rev* 126:1306–1322
- Lajoie FA (1976) On the direction of movement of tropical cyclones. *Aust Meteorol Mag* 24:95–104
- Ma L, Qin Z, Duan Y (2002) Case study on the impact of atmospheric baroclinicity to the initial development of Jianghuai cyclones. *Acta Oceanol Sin* 24:95–104
- Marks DG (1992) The beta and advection model for hurricane track forecasting. NOAA Tech. Memo. NWS NMC 70, Natl. Meteorological Center, Camp Springs, Maryland, p 89
- Mecikalski JR, Tripoli GJ (1998) Inertial available kinetic energy and the dynamics of tropical plume formation. *Mon Weather Rev* 126:2200–2216
- Pasch RJ, Blake ES, Cobb HD III, Roberts DP (2006) Tropical cyclone report—Hurricane Wilma. National Hurricane Center. Retrieved from <http://www.nhc.noaa.gov>
- Pielke RA Jr, Gratz J, Landsea CW, Collins D, Saunders M, Musulin R (2008) Normalized hurricane damages in the United States: 1900–2005. *Nat Hazards Rev* 9:29–42
- Rhyme JR (2007) Technical summary of the National Hurricane Center Track and Intensity Models. Updated September 12, 2007. Available on <http://www.nhc.noaa.gov/modelsummary.shtml>

- Rossby C-G (1949) On a mechanism for the release of potential energy in the atmosphere. *J Meteorol* 6:164–180
- Shapiro LJ (1996) The motion of Hurricane Gloria: A potential vorticity diagnosis. *Mon Weather Rev* 124:2497–2508
- Shapiro LJ, Franklin JL (1998) Potential vorticity asymmetries and tropical cyclone motion. *Mon Weather Rev* 127:124–131
- Shapiro LJ, Ooyama KV (1990) Barotropic vortex evolution on a beta plane. *J Atmos Sci* 47:170–187
- Smith RK (1991) An analytic theory of tropical cyclone motion in a barotropic shear flow. *Q J R Meteorol Soc* 117:685–714
- Smith RK, Ulrich W (1990) An analytical theory of tropical cyclone motion using a barotropic model. *J Atmos Sci* 47:1973–1986
- Smith RK, Weber H (1993) An extended analytic theory of tropical-cyclone motion in a barotropic shear flow. *Q J R Meteorol Soc* 119:1149–1166
- Smith RK, Ulrich W, Sneddon G (2000) On the dynamics of hurricane-like vortices in vertical-shear flows. *Q J R Meteorol Soc* 126:2653–2670
- Wu C-C, Emanuel KA (1995a) Potential vorticity diagnosis of hurricane movement. Part I: a case study of Hurricane Bob (1991). *Mon Weather Rev* 123:69–92
- Wu C-C, Emanuel KA (1995b) Potential vorticity diagnosis of hurricane movement. Part II: Tropical Storm Ana (1991) and Hurricane Andrew (1992). *Mon Weather Rev* 123:93–109
- Wu C-C, Kurihara Y (1996) A numerical study of the feedback mechanisms of hurricane–environment interaction on hurricane movement from the potential vorticity perspective. *J Atmos Sci* 53:2264–2282
- Wu L-G, Wang B (2001) A potential vorticity tendency diagnostic approach for tropical cyclone motion. *Mon Weather Rev* 128:1899–1911
- Zhang F, Bei N, Rotunno R, Snyder C, Epifanio CC (2007) Mesoscale predictability of moist baroclinic waves: convection-permitting experiments and multistage error growth dynamics. *J Atmos Sci* 64:3579–3594